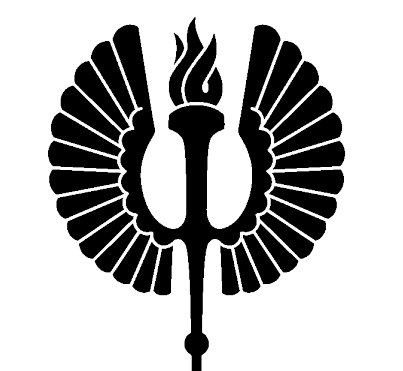




# Self-consistent plasma simulations of particle acceleration and radio emission in the SEPServer project



R. Vainio<sup>1</sup>, A. Afanasiev<sup>1</sup>, M. Battarbee<sup>2</sup>, U. Ganse<sup>1</sup>, A. Kempf<sup>3</sup>,  
P. Kilian<sup>3</sup>, A. Pönni<sup>1</sup>, and F. Spanier<sup>3</sup>

<sup>1</sup>University of Helsinki, FINLAND, <sup>2</sup>University of Turku, FINLAND,  
<sup>3</sup>Julius-Maximilians-Universität Würzburg, GERMANY



## Abstract

Self-consistent plasma simulations in the framework of the SEPServer project were designed to aid the interpretation of the observational results obtained from the analysis of the SEP events. We considered the acceleration of ions and electrons in coronal shocks, the acceleration of electrons in coronal current sheets and the radio emission through the plasma emission mechanism upstream of coronal shocks. Ion transport and acceleration was modeled under the quasi-linear approximation, i.e., as resonant interaction between the charged particles and the Alfvénic fluctuations carried by a prescribed large-scale plasma flow, using the Coronal Shock Acceleration (CSA) code and a new code developed in the framework of SEPServer. Electron acceleration and radio emission was simulated using local plasma simulations making use of the Particle-in-Cell code **ACRONYM**. Here we present a summary of the simulation work performed in SEPServer.

## Shock model in the CSA

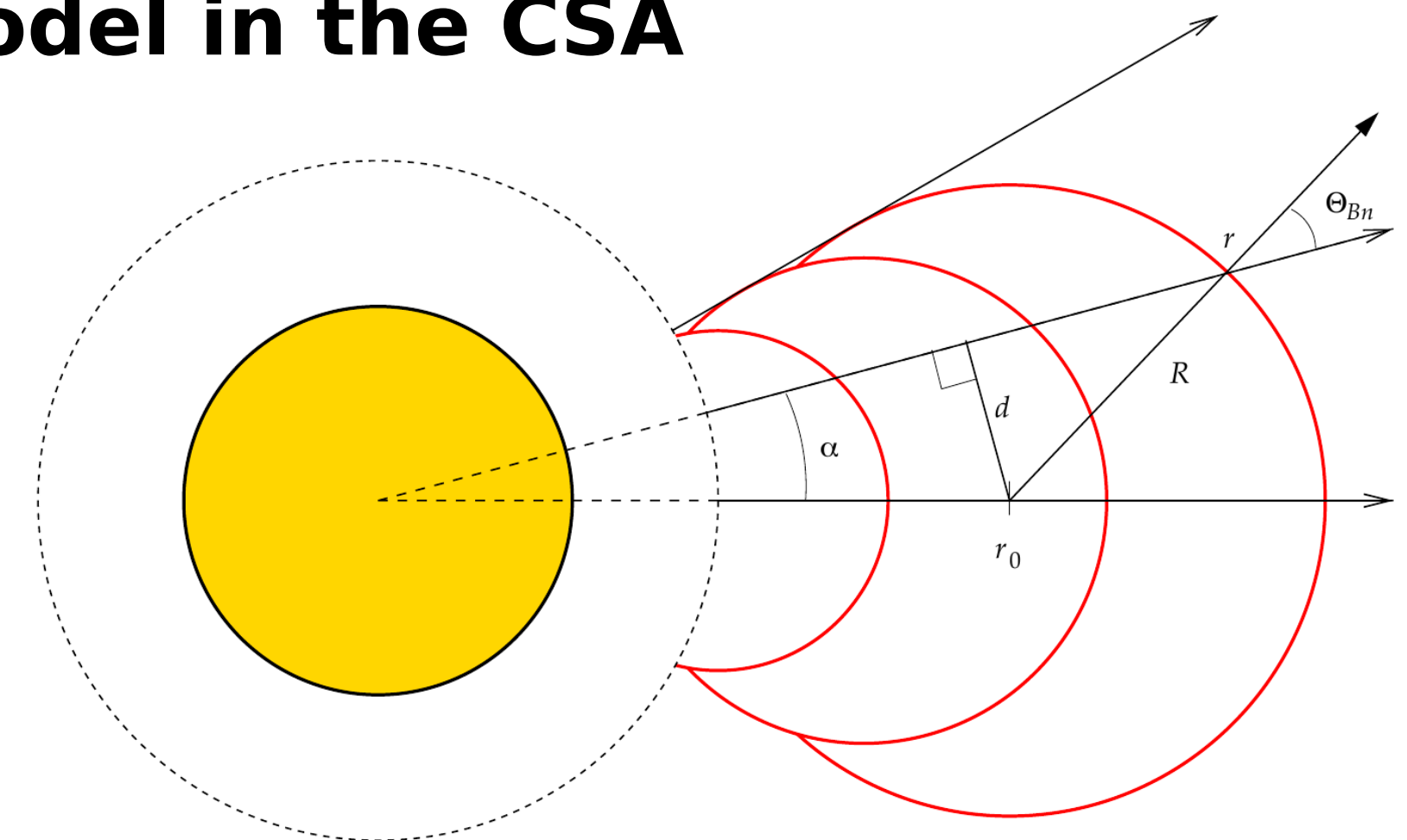


Fig. 1. The global shock model used to determine parameters in the CSA runs. The shock wave consists of an arc of a circle that has its centre point at  $r_0(t)$  propagating at fixed speed and a radius  $R(t)$  scaling with  $r_0(t)$  and leading to self-similar expansion. This gives a constant speed of the shock and a constant shock-normal angle over the simulation.

## Acceleration and transport of ions with the CSA

### Study of the particle injection at a shock

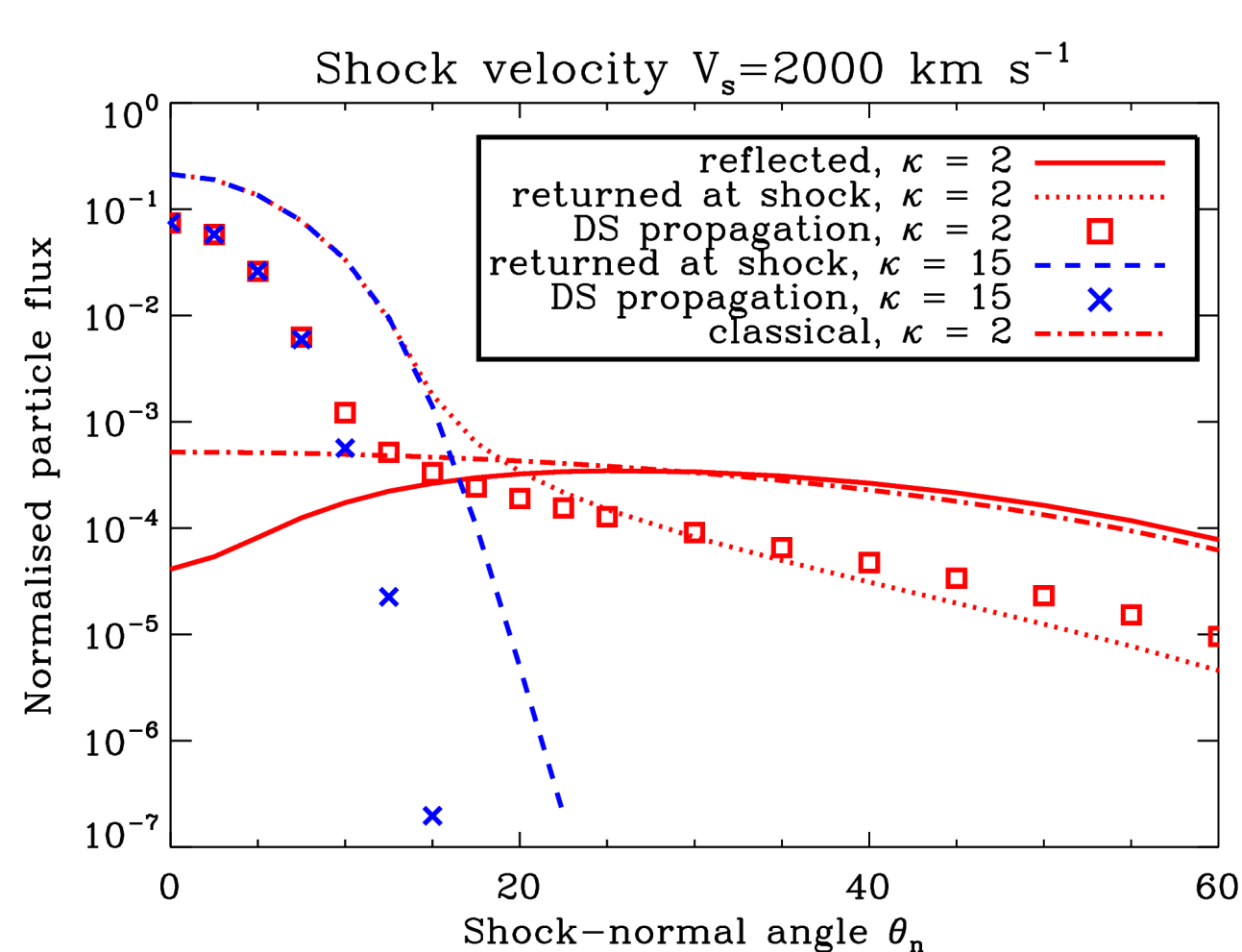


Fig. 2. Flux of injected particles at a shock with  $V_s=2000$  km/s: Data points (square, cross) display the flux returned to the upstream after downstream Monte Carlo propagation. Curves represent injection without downstream propagation. For comparison, the dash-dotted curve displays the integrated flux of all particles that are faster than the classical injection threshold  $v > u_1$ . Seed particles are distributed according to kappa distribution. Results are shown for  $\kappa=2$  (red) and  $\kappa=15$  (blue; reflected particle fluxes and the classical comparison are too low to be visible) (from **Battarbee et al. 2013, A&A, 558, A110**).

### Foreshock formation

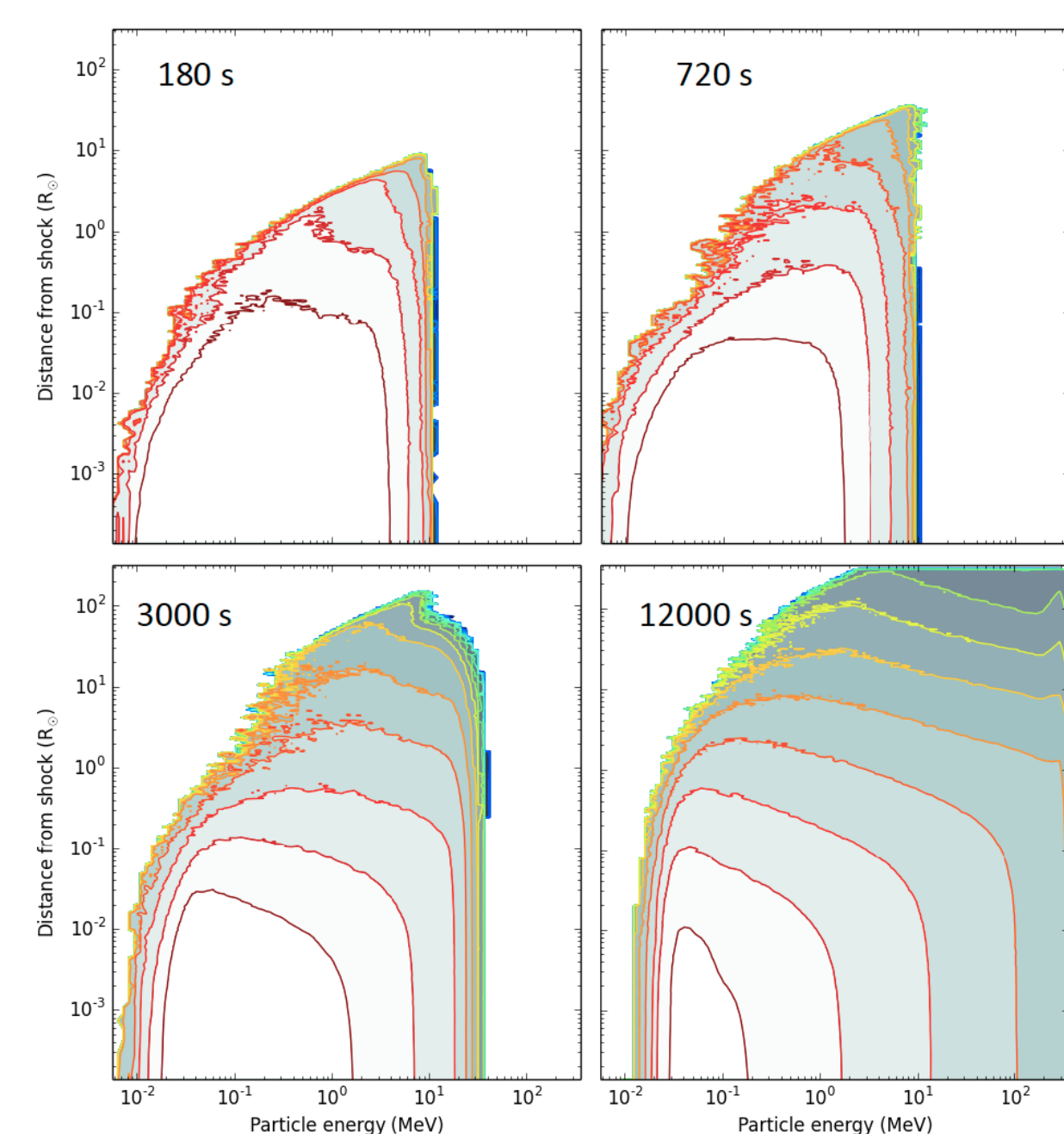


Fig. 3. Simulated differential intensity of the shock-accelerated ions upstream of a coronal shock as a function of position and energy for four different times ( $t = 180; 720; 3000; 12000$  s). The unit of the intensity is protons/( $\text{cm}^2 \text{sr s MeV}$ ). See also the poster by R. Vainio et al. on a semi-analytical foreshock model, # 2919640.

## Implementation of the full resonance condition

### Transport of flare-generated protons in an open magnetic flux tube

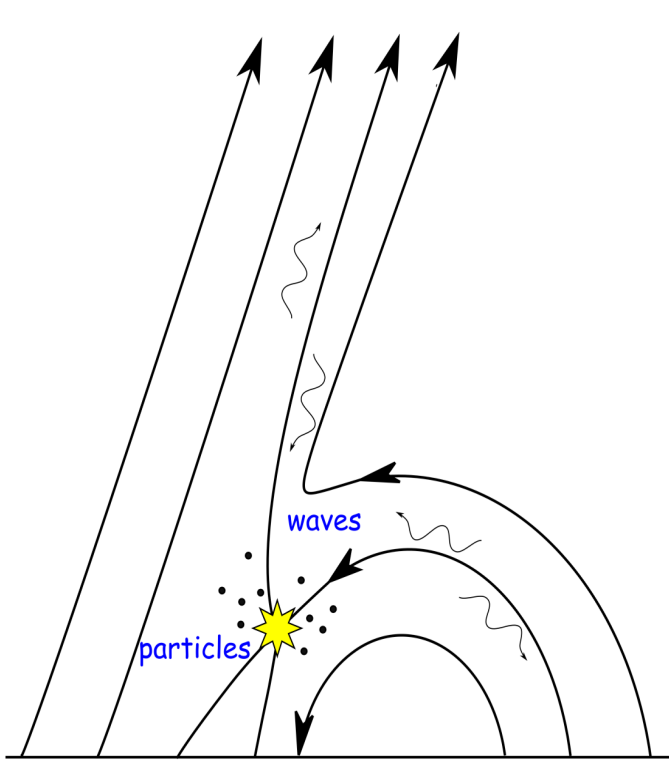


Fig. 4. Physical situation underlying this set of simulations

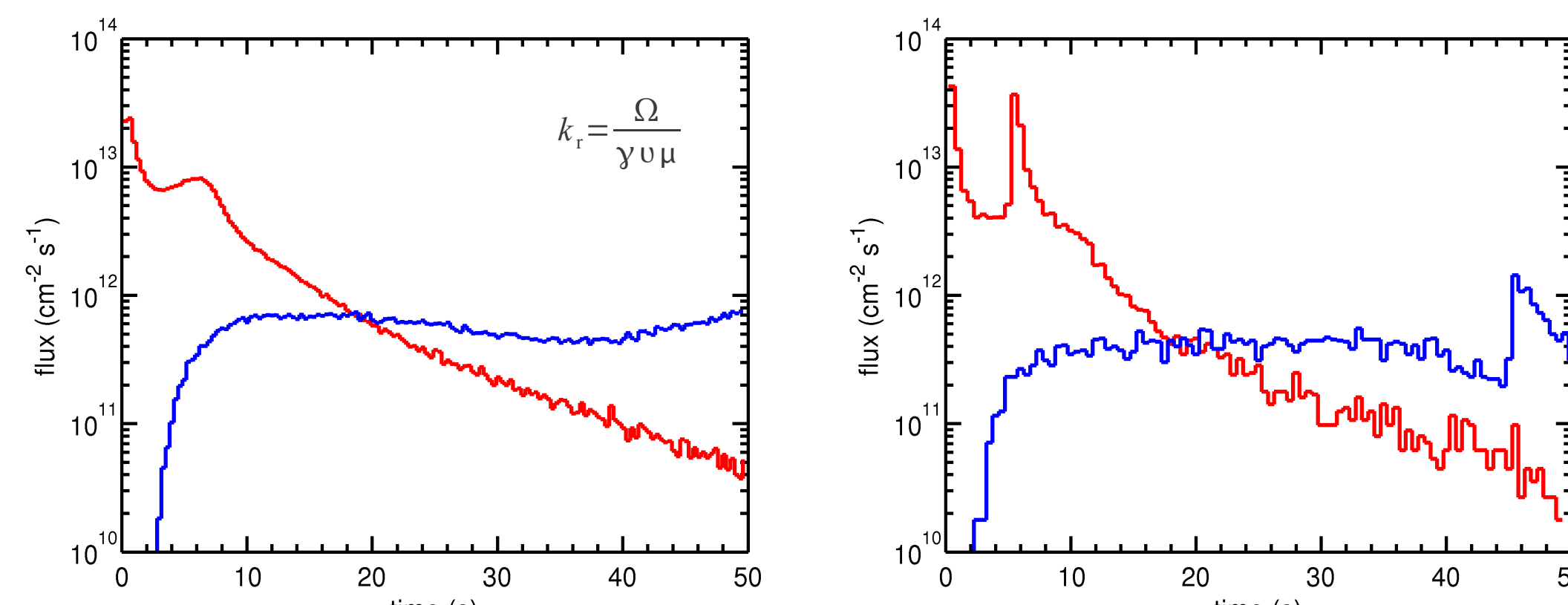


Fig. 5. Fluxes of protons precipitating (red) and escaping into the interplanetary medium (blue). *Left panel:* results obtained using the full resonance condition-based model, *right panel:* results obtained with the simplified resonance condition (from **Afanasiev & Vainio 2013, ApJS, 207, 29**).

### Stochastic re-acceleration of protons in the shock's downstream region

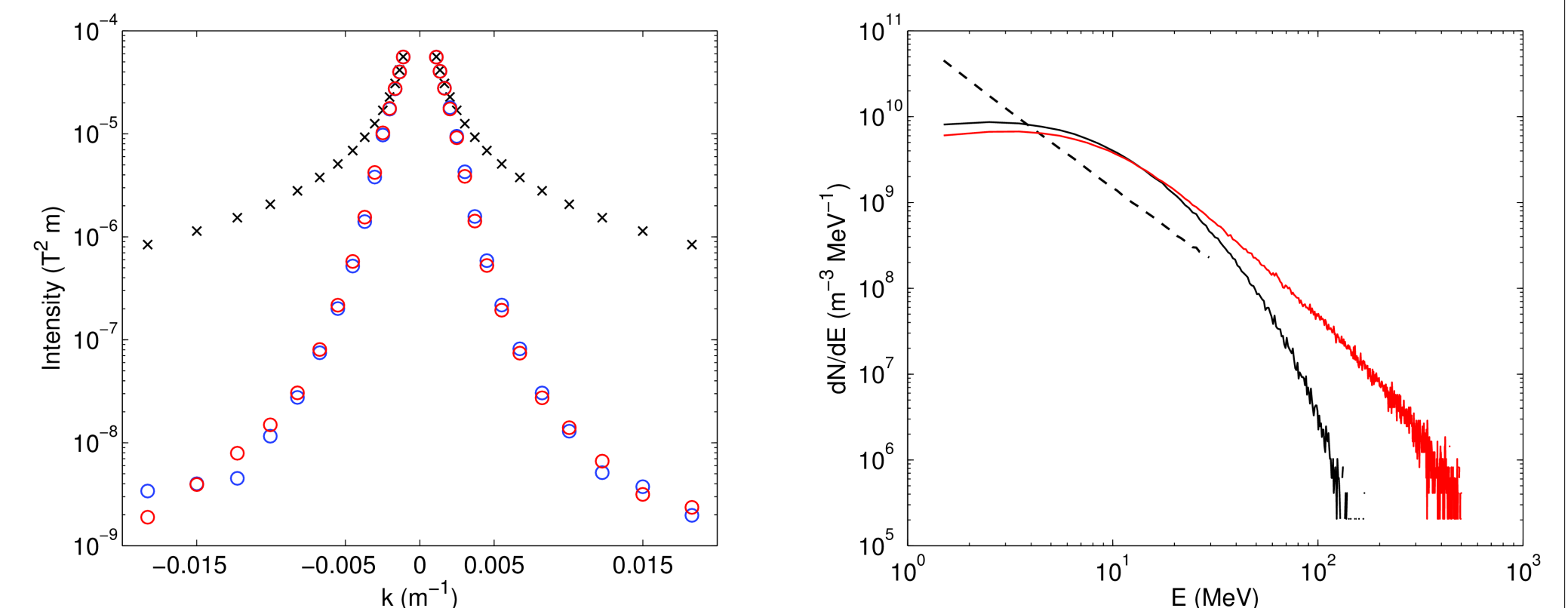


Fig. 6. *Left:* Simulated Alfvén wave spectra (blue and red circles) and the initial Alfvén wave spectrum (black crosses). *Right:* Simulated proton energy spectra (red and black curves) together with the initial spectrum (dashed black line). For more details, see the poster by A. Afanasiev & R. Vainio, # 2919246.

## Radio emission simulations with a PiC code

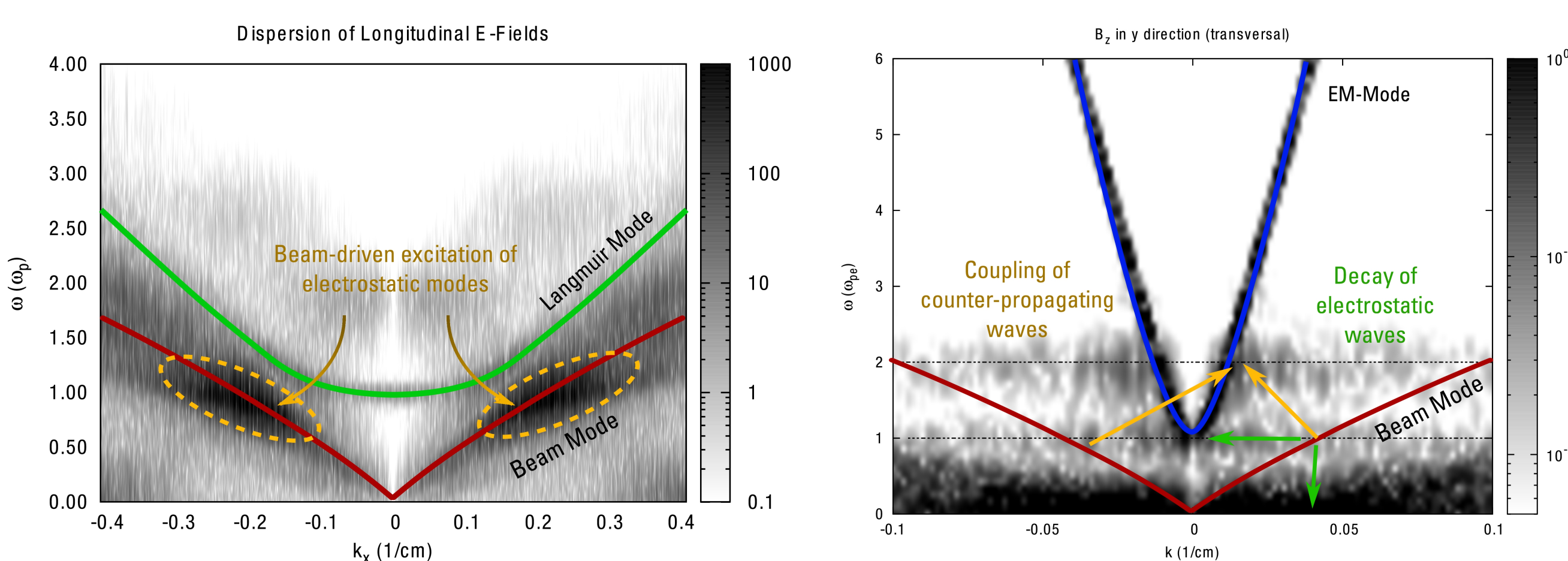


Fig. 7. Wave intensities in  $k$ - $\omega$  space, for longitudinal electrostatic fields (*left*) and transverse electromagnetic fields (*right*). Over that, the theoretical dispersion curves of analytically predicted, regular plasma modes are plotted, and arrows showing the prediction of nonlinear interactions and -decay of electrostatic wave energy into electromagnetic modes (from **Ganse et al. 2013, ApJ, 751, 145**). Electron acceleration in shocks and reconnection regions was simulated using a PiC code as well.

## PiC simulations of shock waves and reconnecting regions

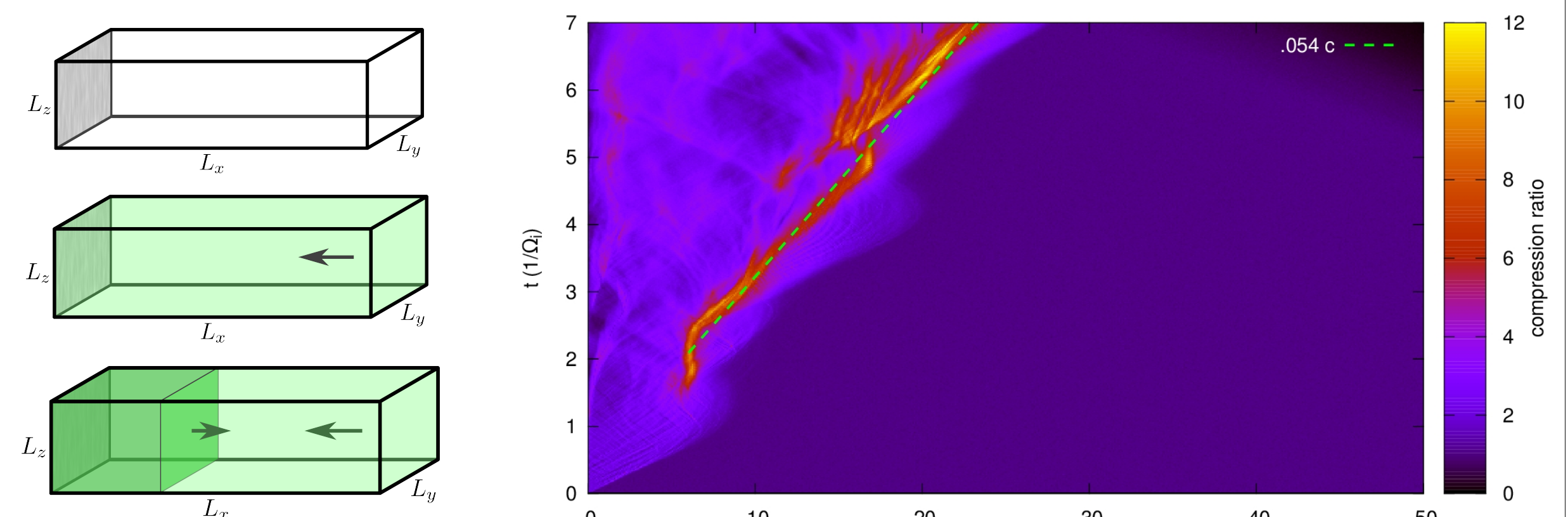
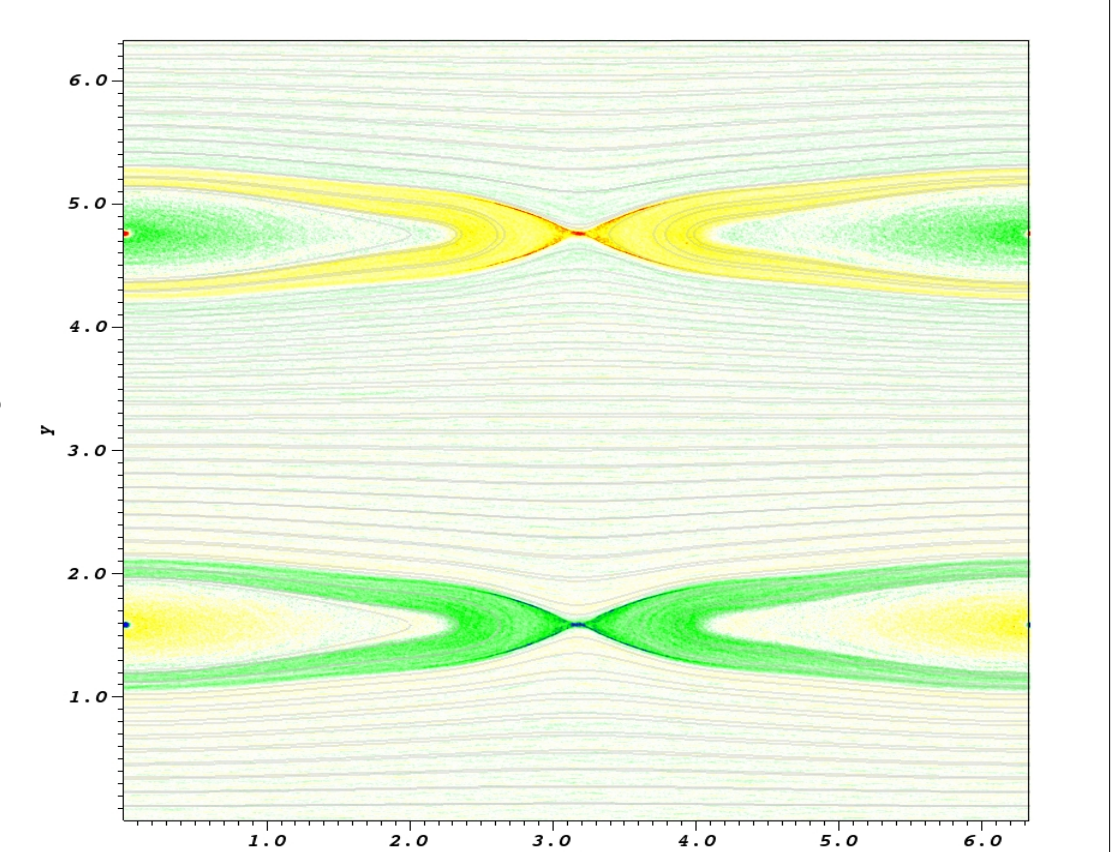


Fig. 8. *Left:* Setup for the shock simulations (from top to bottom). The left side of the simulation box is a conducting wall. Plasma is streaming in from the right and is reflected on the wall. The counter-streaming plasma will produce a shock. *Right:* Evolution of the plasma mass density in the  $x$ - $t$ -plane.

Fig. 9. Out-of-plane electron current density during a 2D simulation of magnetic reconnection. The gray lines are the magnetic field lines. The units along the  $x$ - and  $y$ -direction are ion Inertial lengths.



The research leading to these results has received funding from the European Union Seventh Framework Programme (FP7/2007-2013) under the Grant Agreement no. 262773 (SEPServer).